cmgh
CELLULAR AND MOLECULAR GASTROENTEROLOGY AND HEPATOLOGY

ORIGINAL RESEARCH

NTCP Deficiency Causes Gallbladder Abnormalities in Mice and Human Beings

Fengfeng Mao,[1,2,*] Meng-Xuan Wang,[3,4,*] Xinfeng Hou,[2,5,*] Zhongmin Zhou,[1,2] Yan-Yan Yan,[4] Ling-Juan Fang,[6] Zexi Tan,[2] Wei-Yuan Fang,[4] Teng Liu,[4] Wenhui He,[2] Cong Li,[2,5] Xin-Bao Xie,[4] Shi-Qi Lu,[4] Jianhua Sui,[1,2,7] Fengchao Wang,[2,7] Jun Han,[8,9] Jian-She Wang,[4] and Wenhui Li[2,7]

[1]*School of Life Sciences, Beijing Normal University, Beijing, China;* [2]*National Institute of Biological Sciences, Beijing, China;* [3]*Department of Pediatrics, Jinshan Hospital of Fudan University, Shanghai, China;* [4]*The Center for Pediatric Liver Diseases, Children's Hospital of Fudan University, Shanghai, China;* [5]*School of Life Sciences, Peking University, Beijing, China;* [6]*Department of Pediatric Gastroenterology, the Second Affiliated Hospital, Yuying Children's Hospital of Wenzhou Medical University, Wenzhou, China;* [7]*Tsinghua Institute of Multidisciplinary Biomedical Research, Tsinghua University, Beijing, China;* [8]*University of Victoria-Genome British Columbia Proteomics Centre,* [9]*Division of Medical Sciences, University of Victoria, Victoria, British Columbia, Canada*

Sodium taurocholate co-transporting polypeptide (NTCP, encoded by *SLC10A1*) is a bile acid transporter that also is known to serve as an entry receptor for both the hepatitis B virus and the hepatitis D virus.[1,2] The first reported NTCP knockout (*Slc10a1*$^{-/-}$) mice showed a hypercholanemia phenotype to varying degrees (ie, increased serum bile acid concentrations), but did not show obvious liver injury or other anatomic abnormalities.[3] In human beings, genetic variation in *NTCP* causes hypercholanemia in neonates, but their total bile acid (TBA) levels tend to decrease as age increases.[3–6] Here, we made an overall pathologic examination of hypercolanemic *Slc10a1*$^{-/-}$ mice, and found that their gallbladders had multiple abnormalities throughout their life spans. Importantly, such gallbladder abnormalities also were detected in human infants and teenagers with the NTCP p.Ser267Phe variant.

We examined organs including the liver, small intestine, large intestine, kidney, pancreas, and spleen in 4-week-old and aged *Slc10a1*$^{-/-}$ mice, and found that there were no obvious abnormalities in these organs in the *Slc10a1*$^{-/-}$ mice (Figure 1). However, we observed that *Slc10a1* deficiency caused multiple abnormal phenotypes of the gallbladder: thickened gallbladder walls, enlarged gallbladders (with thickened walls), enlarged gallbladders with blackish green bile, Phrygian cap deformity in its fundus, and small rod-like gallbladders with thickened walls. Note that these phenotypes were present in both male and female *Slc10a1*$^{-/-}$ mice at 4 weeks of age (Figure 2*A–D* and Figure 3*A* and *B*). Histologic analysis showed that *Slc10a1*$^{-/-}$ mice had thickened gallbladder walls, enhanced proliferation of the epithelium, elongated epithelial folds, increased stromal granulocyte infiltration, and submucosal vasodilation (Figure 2*E–L*). Notably, the gallbladder weights were significantly higher in *Slc10a1*$^{-/-}$ mice than in littermate control wild-type (WT) mice (Figure 2*M*). Choi et al[7] in 2006 reported that the fibroblast growth factor (FGF) family protein FGF15 stimulates the enlargement of gallbladders in mice. We thus investigated whether FGF15 may contribute to the observed gallbladder enlargement phenotype among others in the *Slc10a1*$^{-/-}$ mice. Ileal *Fgf15* expression was induced significantly, and correlated positively with serum TBA levels in *Slc10a1*$^{-/-}$ mice and with gallbladder weight (Figure 3*C–E*). Therefore, increased ileal *Fgf15* expression apparently contributes functionally to the gallbladder enlargement phenotype in hypercholanemic *Slc10a1*$^{-/-}$ mice, a finding that warrants further experimental investigations.

Slc10a1$^{-/-}$ mice had hypercholanemia at 4 weeks, however, there were no visible gallstones observed in the gallbladders (Figure 2*B–D* and Figure 3*A* and *B*). Although bile inside the gallbladders of a small proportion of the *Slc10a1*$^{-/-}$ mice was notably more turbid than gallbladder bile of WT mice (Figure 2*N*), a polarizing microscopy-based inspection of bile showed no obvious cholesterol monohydrate crystals (data not shown). We also found that the gallbladder levels of phospholipids increased significantly in *Slc10a1*$^{-/-}$ mice; no differences were observed for gallbladder cholesterol or bile acids levels (Figure 3*F–H*). Consistently, *Slc10a1*$^{-/-}$ mice had significantly lower bile cholesterol saturation index values compared with WT mice ($P < .0001$) (Figure 3*I*), suggesting that these animals are unlikely to suffer from cholesterol gallstone disease. Comprehensive bile acid (BA) profiling of 33 BA species in these mice was conducted by liquid chromatography tandem mass spectrometry (LC-MS/MS), and only concentration of taurine-conjugated β-muricholic acid (TβMCA) significantly decreased in *Slc10a1*$^{-/-}$ mice compared with WT mice (Figure 2*O*).

*Authors share co-first authorship.

Abbreviations used in this letter: **BA, bile acid; FGF, fibroblast growth factor; LC-MS/MS, liquid chromatography with tandem mass spectrometry; MCA, muricholic acid; NTCP, sodium taurocholate co-transporting polypeptide; TBA, total bile acids; UPLC, ultrahigh-performance liquid chromatography; WT, wild-type.**

Most current article

2352-345X
https://doi.org/10.1016/j.jcmgh.2020.09.001

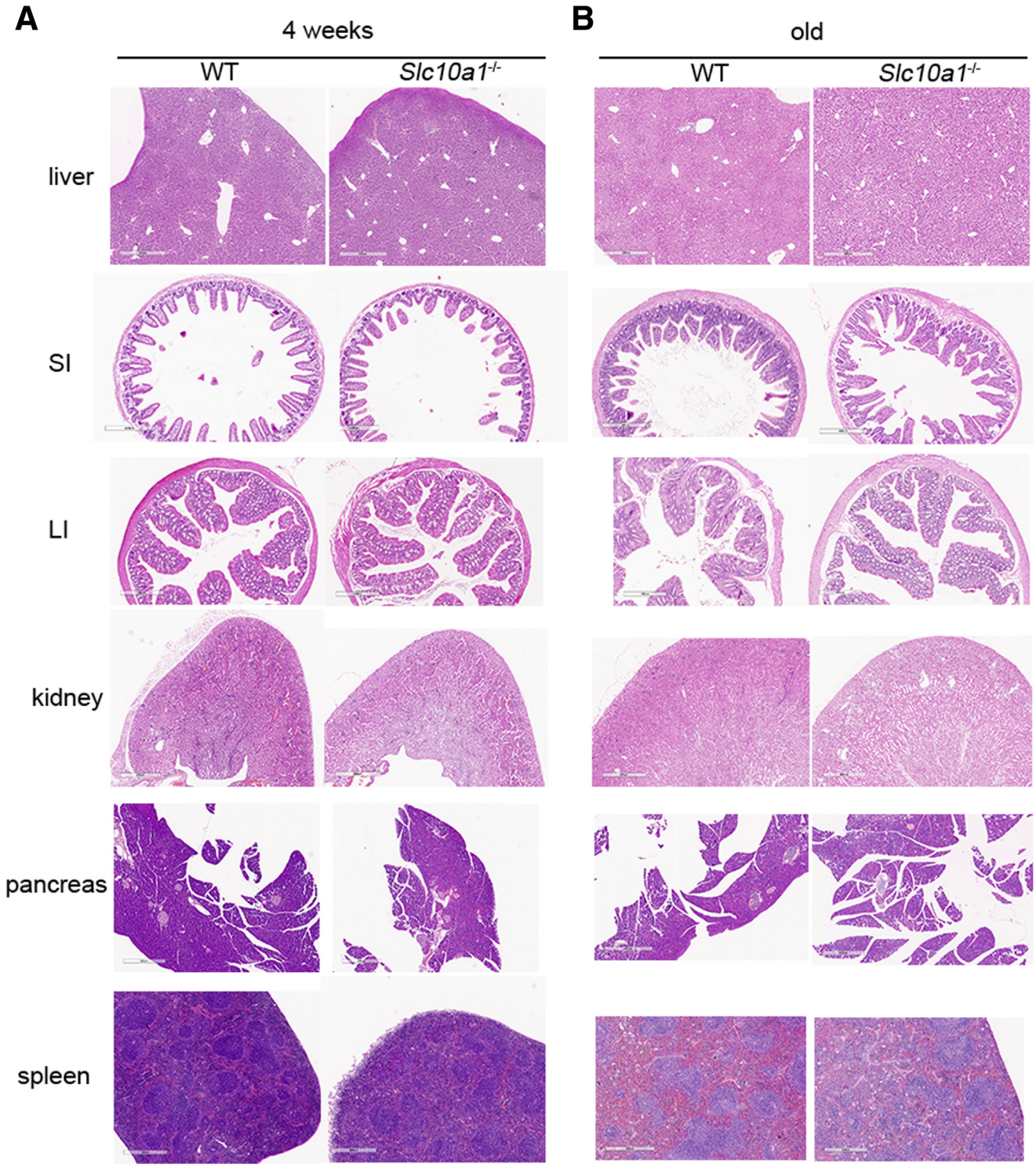

Figure 1. No obvious pathologic changes in 4-week-old and aged *Slc10a1*$^{-/-}$ mice. Representative H&E staining of liver, small intestine (SI), large intestine (LI), kidney, pancreas, and spleen in (*A*) 4-week-old and (*B*) aged WT and *Slc10a1*$^{-/-}$ mice. *Slc10a1*$^{-/-}$ mice with extremely high serum TBA levels (>1 mmol/L) showed mild liver injury and inflammation (not shown).

We recently reported that the overall serum TBA levels tended to decrease gradually with increasing age in *Slc10a1*$^{-/-}$ mice.[5] BA profiling in aged *Slc10a1*$^{-/-}$ mice showed that the concentrations of BAs, including cholic acid, αMCA, βMCA, ωMCA, chenodeoxycholic acid, ursodeoxycholic acid, and their taurine or glycine conjugates are similar to that of aged male or female WT mice, respectively (Figure 4*A* and *B*). However, the aged *Slc10a1*$^{-/-}$ mice still had thickened

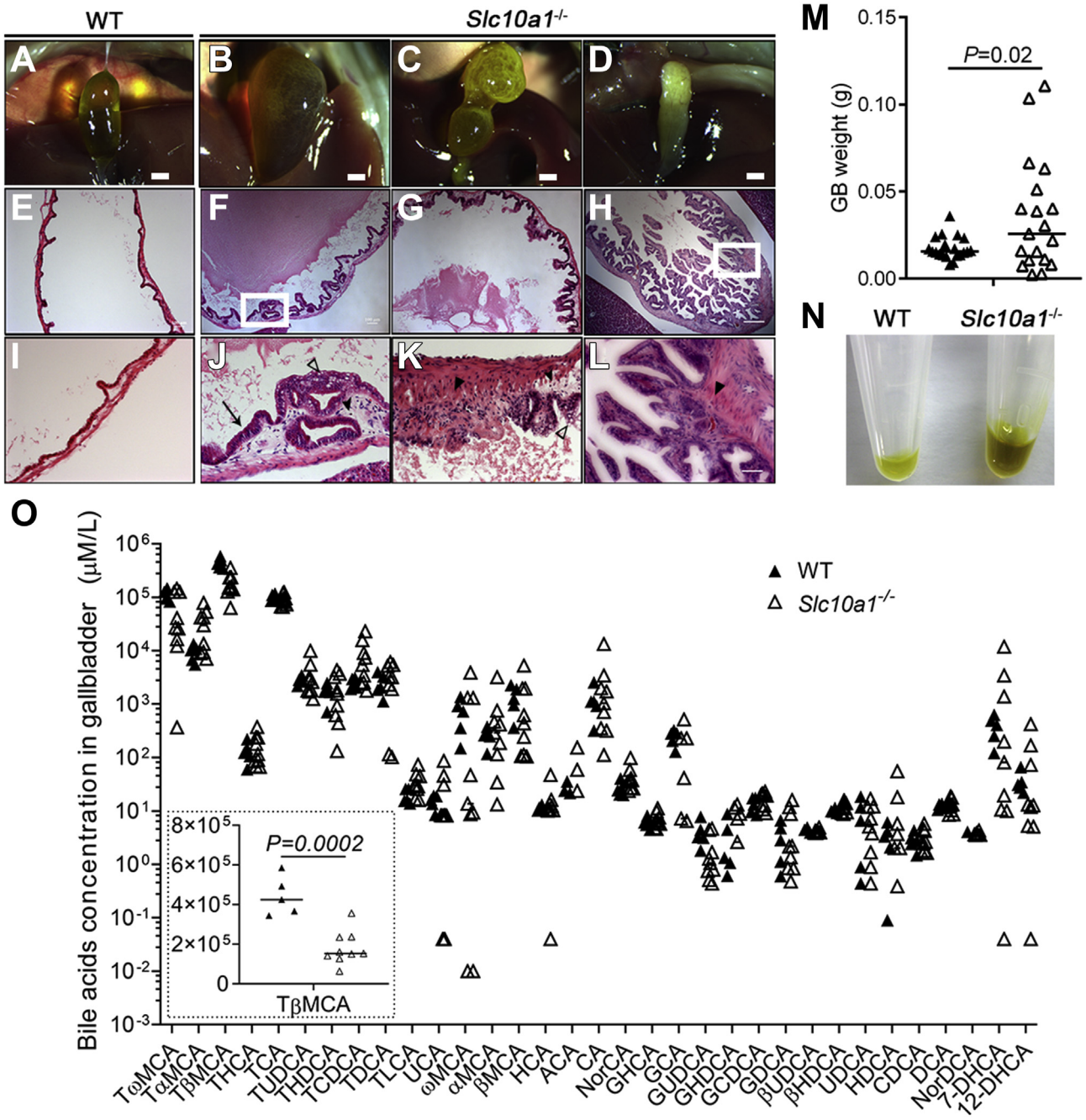

Figure 2. NTCP deficiency causes gallbladder abnormalities in mice. Representative photographs of gallbladders from fasted 4-week-old (*A*) male WT and (*B–D*) *Slc10a1*$^{-/-}$ mice. *Scale bar*: 1 mm. Representative gallbladder H&E staining of (*E* and *I*) WT mice related to panel *A*, and (*F-H* and *J-L*) *Slc10a1*$^{-/-}$ mice related to panels *B-D*, respectively. The *arrow* indicates elongated epithelial folds, *arrowheads* indicate stromal granulocyte infiltration, *closed triangles* indicate submucosal vasodilation, and *open triangles* indicate the presence of lipids in the gallbladder walls. (*M*) Gallbladder (GB) weights in WT (n = 20) and *Slc10a1*$^{-/-}$ mice (n = 19) at 4 weeks of age. (*N*) Representative photos of bile from WT and *Slc10a1*$^{-/-}$ mice. (*O*) BA profiling in bile from WT and *Slc10a1*$^{-/-}$ mice (WT, n = 5; *Slc10a1*$^{-/-}$, n = 9) at 4 weeks of age. *Inset*: the significant decrease of taurine-conjugated β MCA (TβMCA). All mice were male. Values are shown as medians. Each *symbol* represents an individual mouse. Two-tailed Student *t* tests were used.

gallbladder walls, or even a completely filled gallbladder cavity by the age of 20 months (Figure 4*C*). Furthermore, no significant changes in bile flow and biliary excretion of BAs were observed between aged WT and *Slc10a1*$^{-/-}$ mice, although *Slc10a1*$^{-/-}$ mice showed a trend toward slightly increased bile flow (Figure 4*D* and *E*).

To determine whether loss of NTCP function also can lead to gallbladder abnormalities in human beings, we

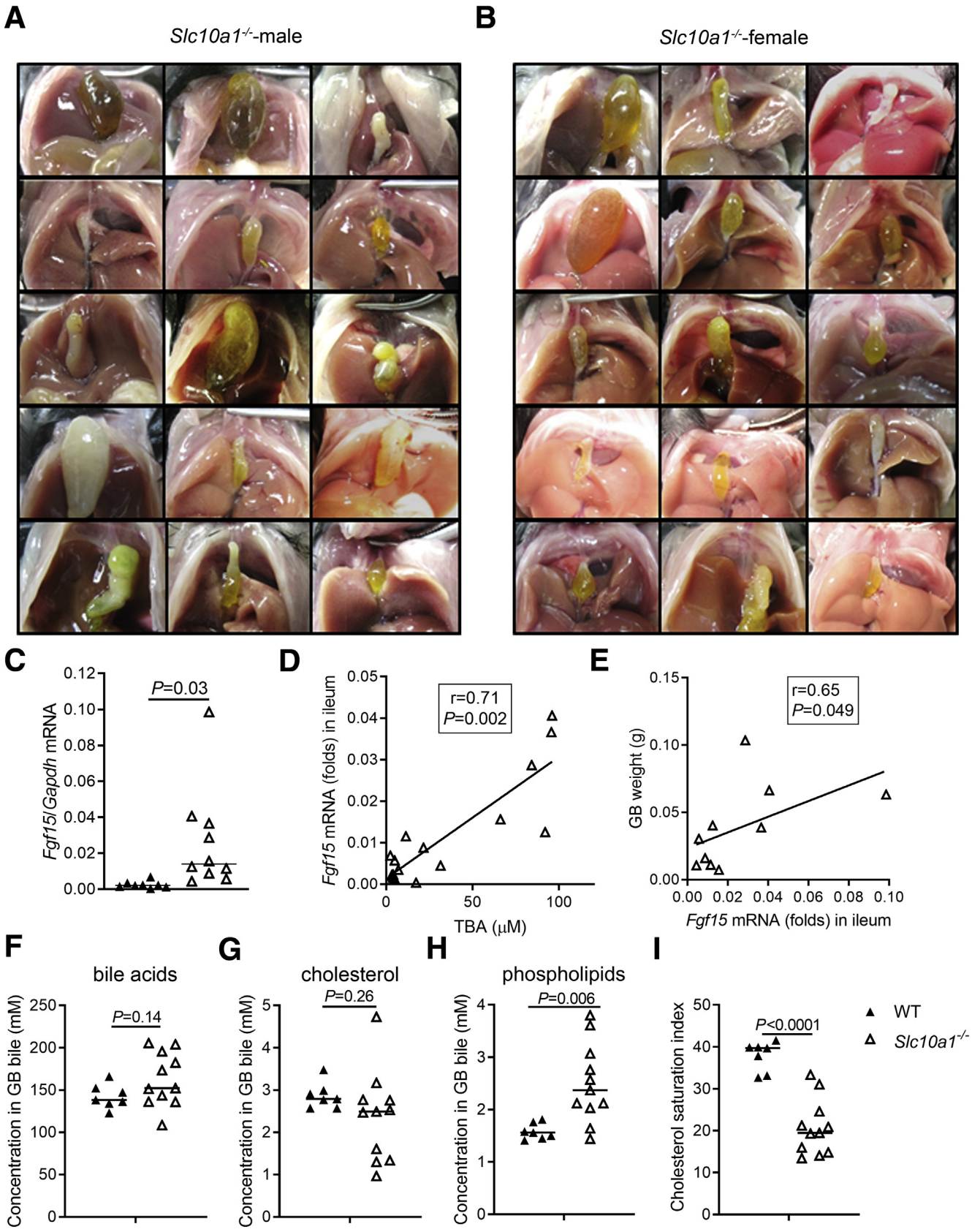

Figure 3. *Slc10a1*$^{-/-}$ mice did not develop cholesterol gallstone disease. Demonstrations of gallbladder abnormalities in 4-week-old (*A*) male and (*B*) female *Slc10a1*$^{-/-}$ mice. (*C*) Ileal *Fgf15* expression in male WT (n = 8) and *Slc10a1*$^{-/-}$ mice (n = 10) at 4 weeks of age. (*D*) Correlation of ileal *Fgf15* expression and TBA level in male *Slc10a1*$^{-/-}$ mice (n = 17). (*E*) Correlation of ileal *Fgf15* expression and gallbladder weight in male *Slc10a1*$^{-/-}$ mice (n = 10). Concentrations of (*F*) bile acids, (*G*) cholesterol, and (*H*) phospholipids in GB bile, and (*I*) values of cholesterol saturation index in WT (n = 7) and *Slc10a1*$^{-/-}$ mice (n = 11) at 4 weeks of age. Values are given as medians. Each symbol represents an individual mouse. Two-tailed Student *t* tests and Spearman rank correlation analysis were used. mRNA, messenger RNA.

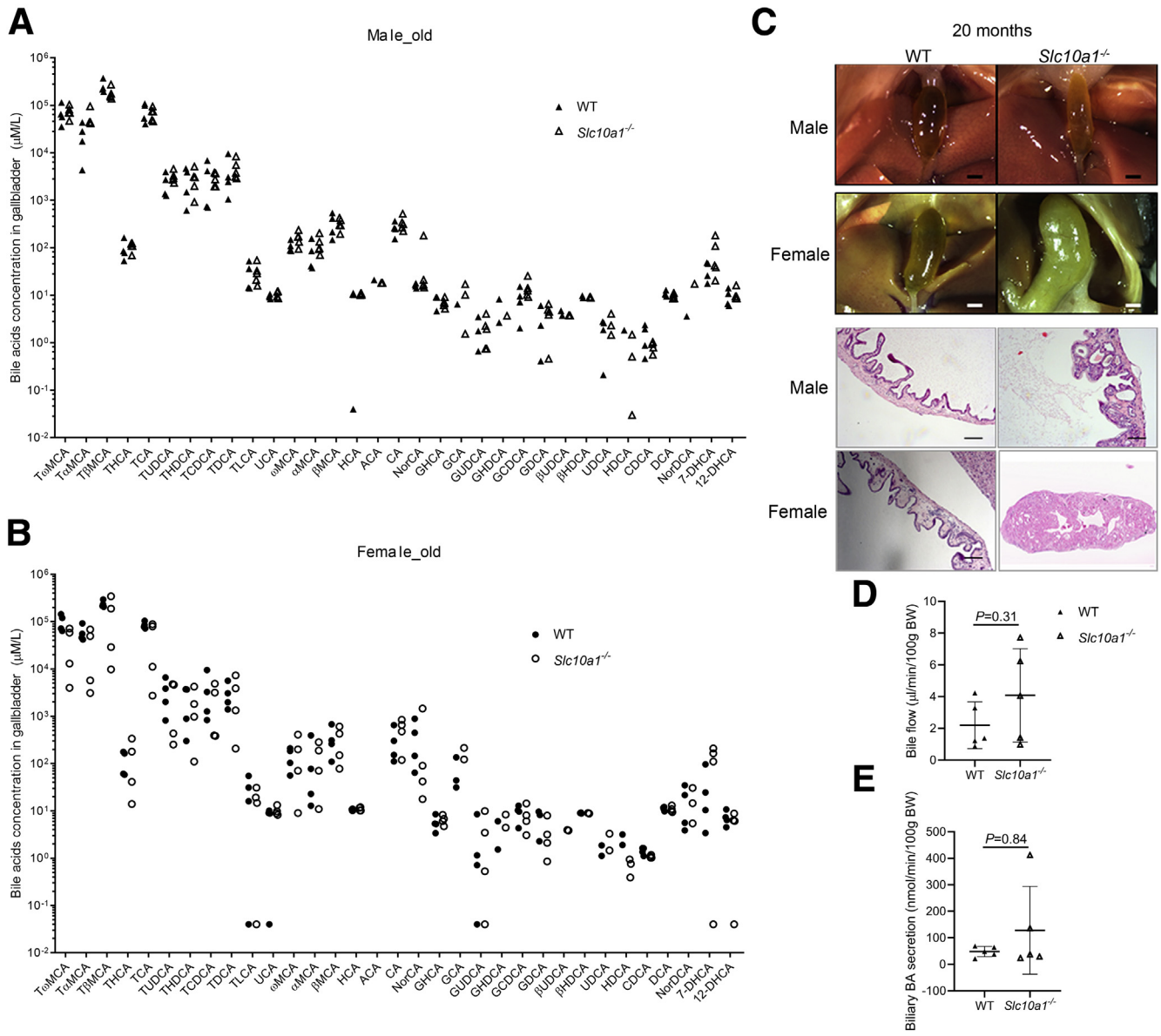

Figure 4. Gallbladder abnormalities in aged *Slc10a1*$^{-/-}$ mice. BA profiling in bile from old (*A*) male and (*B*) female WT and *Slc10a1*$^{-/-}$ mice (n = 4–5). (*C*) Representative photographs and H&E staining of gallbladder abnormalities in old male and female *Slc10a1*$^{-/-}$ mice. (*D*) Bile flow and (*E*) biliary BA secretion during the 10-minute collection period for WT and *Slc10a1*$^{-/-}$ mice (n = 5). Values are shown as mean ± SD. Each symbol represents an individual mouse. Two-tailed Student *t* tests were used.

conducted a retrospective analysis of 33 individuals with the NTCP p.Ser267Phe variant who we recently examined in a clinical study of young children showing abnormal TBA levels.[5,11] Ultrasound examination of 2 teenagers (ages, 14–15 y) with this mutation showed obvious gallbladder polyps (Figure 5*A* and *B*); 2 infants (ages, 6–7 mo) also showed gallbladders containing either 1 large gallstone or multiple sand-like gallstones (Figure 5*C* and *D*). Beyond confirming our suppositions based on the gallbladder phenotypes of the *Slc10a1*$^{-/-}$ mice, these findings indicate that human beings with the NTCP p.Ser267Phe variant are at risk for developing gallbladder abnormalities. Indeed, a Fisher exact test–based analysis of the prospective cohorts showed that such individuals develop gallbladder abnormalities at significantly higher rates than 2 other inherited liver diseases: Wilson disease and glycogen storage disease (4 of 33 vs 0 of 174, respectively; $P < .001$) (Table 1).

The BA composition in plasma of NTCP p.Ser267Phe variants with gallbladder abnormalities is changed significantly (Figure 5*E*).[5] However, no significant changes in serum levels of FGF19, the human ortholog of FGF15, were observed between healthy controls and NTCP p.Ser267Phe variants, although these variants showed a trend toward slightly increased serum FGF19 levels ($P = .22$) independent of the TBA levels (Figure 5*F* and *G*).[6,8] Thus, NTCP

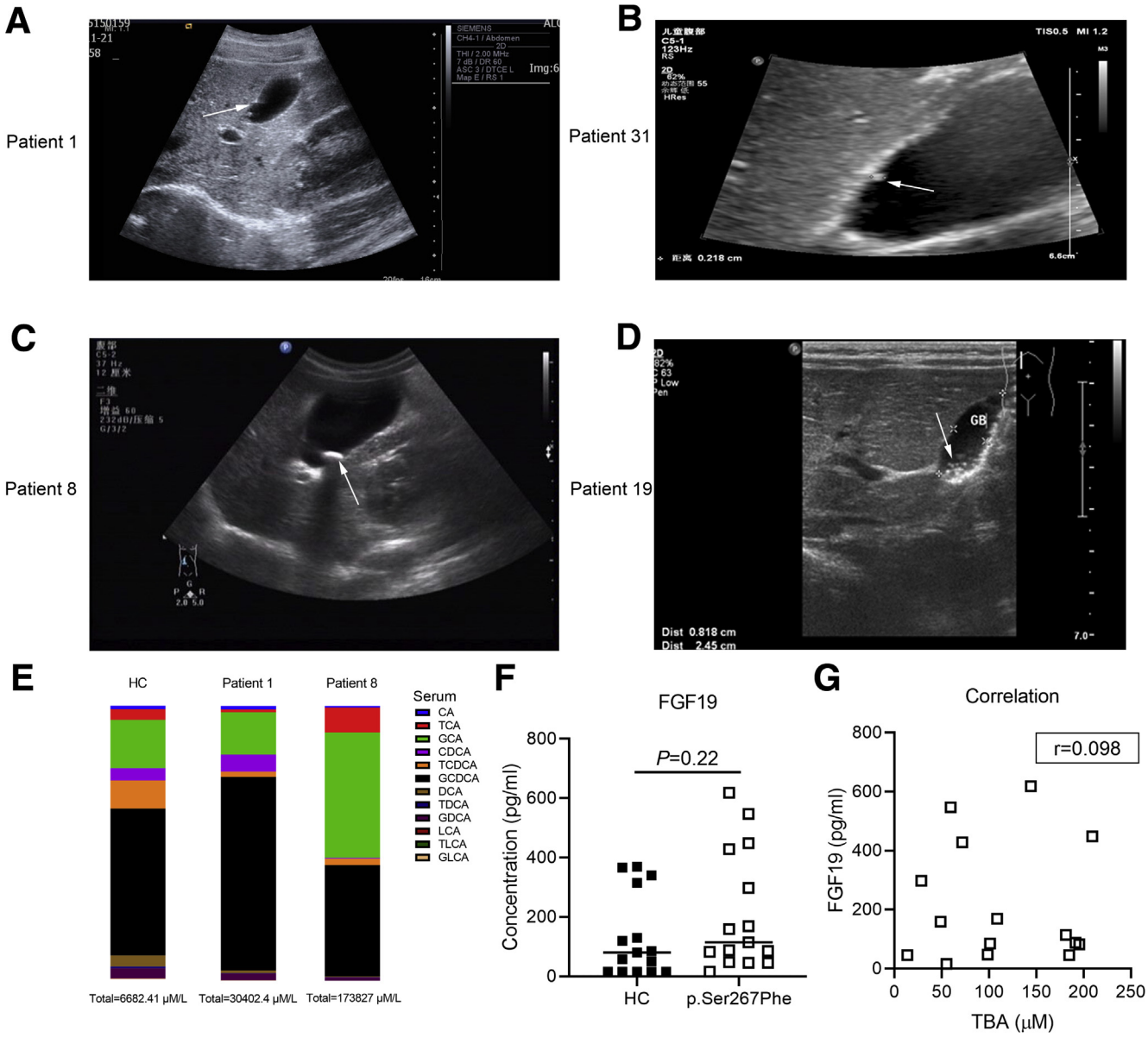

Figure 5. Infant and teenage human beings with the NTCP p.Ser267Phe variant present with gallbladder abnormalities. Abdominal ultrasound indicated the following: (*A*) multiple polyps in the gallbladder (maximal diameter, approximately 5 mm), male, age 15 years; (*B*) a polyp in the gallbladder (diameter, approximately 2 mm), male, age 14 years; (*C*) a gallstone in the gallbladder (size, 1.1 cm ◇ 0.6 cm), male, age 6 months; and (*D*) a rough gallbladder wall and multiple sand-like gallstones in the gallbladder (diameters, 0.6–1.3 mm), male, age 7 months. *Arrows* indicate the sites of gallbladder abnormality. (*E*) Major primary and secondary BAs in plasma from healthy controls (HCs, shown with a mean level of each BA species, n = 43), patient 1 and patient 8 by UPLC/multiple-reaction monitoring-MS. (*F*) Sera levels of FGF19 in HCs (n = 15) and NTCP p.Ser267Phe variants (n = 15). (*G*) Correlation of FGF19 levels and TBA levels in NTCP p.Ser267Phe variants. Values are shown as medians. Each symbol represents a HC individual with the NTCP p.Ser267Phe variant. Two-tailed Student *t* test and Spearman rank correlation analysis were used.

deficiency can result in dysregulated gallbladder wall morphology (ie, thickened gallbladder walls or gallbladder polyps) in both mouse and human beings but causes gallstone formation only in human beings.

In conclusion, the present study suggests that deficiency of NTCP in hepatocytes leads to gallbladder abnormalities in both mice and human beings. In addition, and distinct from metabolism phenotypes such as dysregulated TBA levels in infants that later decrease, NTCP deficiency also can lead to gallbladder abnormalities that occur in children that may be irreversible throughout one's life. All of these findings point to NTCP deficiency as a potentially underappreciated cause for gallbladder diseases encountered by physicians in the clinic.[9] Moreover, our study supports that potential

Table 1. Information of Gallbladder Abnormalities in Inherited Liver Diseases

Inherited liver disease	Patient ID	Sex	Date of birth, month/day/year	Date of finding gallbladder abnormality, month/day/year
NTCP S267F (total, 33 patients)	P1	Male	12/14/2000	08/11/2015
	P8	Male	06/11/2012	11/01/2013
	P19	Male	01/30/2017	09/04/2017
	P31	Male	12/14/2004	01/21/2019
Wilson disease (total, 83 patients)	0	–	–	–
Glycogen storage disease (total, 91 patients)	0	–	–	–

gallbladder-related effects should be monitored carefully in ongoing efforts to develop therapies against hepatitis B virus/hepatitis D virus infections that are based on NTCP-related targets.[10]

Materials and Methods

Slc10a1 Knockout Mice

WT and *Slc10a1*$^{-/-}$ mice[5] were housed in specific pathogen-free conditions at the animal facility of the National Institute of Biological Sciences (Beijing, China). Animal experiments were performed in accordance with the National Institute of Biological Sciences institutional regulations after approval by the Institutional Animal Care and Use Committee.

Human Study

To explore the gallbladder conditions in human beings, patients genetically diagnosed with NTCP p.Ser267Phe variant presenting to the Liver Center of Children's Hospital of Fudan University and the Department of Pediatrics at Jinshan Hospital of Fudan University from January 2012 to December 2018 were included for this study.[11] Patients diagnosed with Wilson disease or glycogen storage disease were selected from the hospital's information system as age- and sex-matched controls. The information from gallbladder examination, abdominal ultrasonography and magnetic resonance imaging were picked up. Patients with hepatic failure, hyperuricemia, and nephrotic syndrome, or another disease that may cause edema or ascites, or patients who received a liver transplant were excluded. The study protocol was approved by the Children's Hospital of Fudan University and Jinshan Hospital of Fudan University Ethics Committees at both institutions. Written informed consent was obtained from parents, guardians, and/or patients. Each participant provided written informed consent before participation in accordance with the ethical guidelines of the 1975 Declaration of Helsinki.

H&E Staining

For H&E staining, fresh tissues were rinsed in phosphate-buffered saline and fixed in 4% paraformaldehyde overnight. Sections (5 μm) were deparaffinized, rehydrated, and stained with H&E. Slides were dehydrated, and then were cleared and mounted in neutral balsam. Images were obtained using a Zeiss Axio Imager M1 microscope with an AxioCam HRc camera controlled by AxioVision 4.6 software (Oberkochen, Germany) or Leica Aperio AT2 digital whole slide scanning (Vista, CA). Representative images of at least 3 sample replicates are presented in the figures (Figures 1, 2 and 4).

Analysis of Cholesterol, Phospholipids, and Bile Acids in the Gallbladder Bile

Bile samples were collected using an infusion needle connected to a 1 mL syringe. Cholesterol and phospholipids were measured using enzymatic method kits (Applygen E1005, Beijing, China for cholesterol, and WAKO 296-63801, Osaka, Japan for phospholipids) following the product instructions. Measurement of bile acids from bile samples was conducted commercially by the Beijing Lawke Health Laboratory Center for Clinical Laboratory Development, Inc (Beijing, China). The cholesterol saturation index of bile was calculated as described by Carey.[12]

Bile Acid Profiling

Human BA profiling in plasma was performed by reverse-phase ultrahigh-performance liquid chromatography (UPLC)/multiple-reaction monitoring-mass spectrometry with negative ion detection.[5,13,14] BAs were measured in bile samples that were previously stored at −80°C using a quantitative UPLC-MS/MS platform (ACQUITY UPLC-Xevo TQ-S; Waters Corp, Milford, MA).[15] All bile samples were diluted 1000× before the test. All chromatographic separations were performed with an ACQUITY BEH C18 column VanGuard precolumn (2.1 × 5 mm) and analytical column (2.1 × 100 mm). The elution solvents were water with formic acid (pH, 3.25, A) and acetonitrile/methanol (8:2, B). The flow rate was 400 μL/min with the following mobile phase gradient: 0–0.3 minutes (5% B), 0.3–0.5 minutes (5%–10% B), 0.5–2 minutes (10%–15% B), 2–3 minutes (15%–30% B), 3–6 minutes (30% B), 6–8 minutes (30–35% B), 8–9 minutes (35%–40% B), 9–10 minutes (40% B), 10–15 minutes (40%–75% B), 15–15.5 minutes (75%–100% B), 15.5–16.2 minutes (100% B), 16.2–16.3 minutes (100–5% B), and 16.3–17 minutes (5% B). The cone and collision energy for each BA used the optimized settings from QuanOptimize application manager (Milford, CT). The raw data generated by UPLC-MS/MS then were processed using QuanMET software to perform peak

integration, calibration, and quantitation for each BA. Testing services were provided by Metabo-Profile, Inc (Shanghai, China). Quantified BAs contained 33 species, including cholic acid, chenodeoxycholic acid, tauro ωMCA, tauro αMCA, tauro βMCA, taurocholic acid, glycocholic acid, glycochenodeoxycholate, taurochenodeoxycholate, deoxycholic acid, ursodeoxycholic acid, glycodeoxycholic acid, taurodeoxycholate, glycoursodeoxycholic acid, tauroursodeoxycholic acid, taurohyocholate, taurohyodeoxycholic acid, taurolithocholate, ursocholic acid, ωMCA, αMCA, βMCA, γ-muricholic acid/hyocholic acid, allocholic acid, nor cholic acid, glycohyocholate, glycohyodeoxycholate, 3β-ursodeoxycholic acid, β-hyodeoxycholic acid, α-hyodeoxycholic acid, 23-nordeoxycholic acid, 7-ketodeoxycholic acid, and 12-ketodeoxycholic acid.

Bile Secretion In Vivo

Bile secretion in fasted mice was performed by performing gallbladder cannulation and bile collection for 10 minutes after distal ligation of the common bile duct. Bile flow was determined gravimetrically assuming a density of 1 g/mL for bile. Biliary BA secretion was calculated as the product of the bile flow and the bile concentration in a 10-minute collection period.[3,16]

FGF19 Levels in NTCP p.Ser267Phe Variants

Circulation FGF19 levels of the health controls and NTCP p.Ser267Phe variant were determined using a sandwich enzyme-linked immunosorbent assay according to the manufacturer's instructions (DF1900; R&D Systems, Inc, Minneapolis, MN).[17]

Quantitative Polymerase Chain Reaction Analysis

Freshly isolated ileum samples were washed with phosphate-buffered saline to flush out their content. The cleaned samples were chopped into homogenates on the ice, treated with TRIzol reagent (Carlsbad, CA), and vortexed immediately. Samples in TRIzol were incubated at room temperature ($\sim$25°C) for 5 minutes and stored at -80°C. Extraction of RNA followed the TRIzol product instructions. Quantitative polymerase chain reaction was performed on a 7500 fast instrument (Applied Biosystems, Foster City, CA) using SYBR Green.[18]

Statistical Analysis

Medians are presented in Figures 2, 3 and 5) unless otherwise stated. Inferential statistical significance between 2 groups was examined using 2-tailed Student *t* tests. Correlation between 2 groups of measured parameters was analyzed using Spearman rank correlation analysis implemented in GraphPad Prism (version 6.0, San Diego, CA). The Fisher exact test was performed to compare the difference in gender and disease groups. *P* values less than .05 were considered to indicate statistical significance.

Access to Data

All authors had access to all of the data and reviewed and approved the final manuscript.

References

1. Trauner M, Boyer JL. Bile salt transporters: molecular characterization, function, and regulation. Physiol Rev 2003;83:633–671.
2. Yan H, Zhong G, Xu G, He W, Jing Z, Gao Z, Huang Y, Qi Y, Peng B, Wang H, Fu L, Song M, Chen P, Gao W, Ren B, Sun Y, Cai T, Feng X, Sui J, Li W. Sodium taurocholate cotransporting polypeptide is a functional receptor for human hepatitis B and D virus. eLife 2012;1:e00049.
3. Slijepcevic D, Kaufman C, Wichers CG, Gilglioni EH, Lempp FA, Duijst S, de Waart DR, Oude Elferink RPJ, Mier W, Stieger B, Beuers U, Urban S, van de Graaf SFJ. Impaired uptake of conjugated bile acids and hepatitis b virus pres1-binding in na(+) -taurocholate cotransporting polypeptide knockout mice. Hepatology 2015;62:207–219.
4. Deng M, Mao M, Guo L, Chen F-P, Wen W-R, Song Y-Z. Clinical and molecular study of a pediatric patient with sodium taurocholate cotransporting polypeptide deficiency. Exp Ther Med 2016;12:3294–3300.
5. Mao F, Liu T, Hou X, Zhao H, He W, Li C, Jing Z, Sui J, Wang F, Liu X, Han J, Borchers CH, Wang J-S, Li W. Increased sulfation of bile acids in mice and human subjects with sodium taurocholate cotransporting polypeptide deficiency. J Biol Chem 2019;294:11853–11862.
6. Vaz FM, Paulusma CC, Huidekoper H, de Ru M, Lim C, Koster J, Ho-Mok K, Bootsma AH, Groen AK, Schaap FG, Oude Elferink RP, Waterham HR, Wanders RJ. Sodium taurocholate cotransporting polypeptide (SLC10A1) deficiency: conjugated hypercholanemia without a clear clinical phenotype. Hepatology 2015;61:260–267.
7. Choi M, Moschetta A, Bookout AL, Peng L, Umetani M, Holmstrom SR, Suino-Powell K, Xu HE, Richardson JA, Gerard RD, Mangelsdorf DJ. Identification of a hormonal basis for gallbladder filling. Nat Med 2006;12:1253–1255.
8. Zweers SJLB, Booij KAC, Komuta M, Roskams T, Gouma DJ, Jansen LM, Schaap FG. The human gallbladder secretes fibroblast growth factor 19 into bile: Towards defining the role of fibroblast growth factor 19 in the enterobiliary tract. Hepatology 2012;55:575–583.
9. Dong C, Zhang B-P, Wang H, Xu H, Zhang C, Cai Z-S, Wang D-W, Shu S-N, Huang Z-H, Luo X-P. Clinical and histopathologic features of sodium taurocholate cotransporting polypeptide deficiency in pediatric patients. Medicine (Baltimore) 2019;98:e17305.
10. Schierwagen R, Klein S, Trebicka J. A new treatment for chronic hepatitis B and D offers novel insights into obesity and hepatic steatosis. Cell Mol Gastroenterol Hepatol 2020;10:649–651.
11. Yant YY, Wang MX, Gong JY, Liu LL, Setchell KDR, Xie XB, Wang NL, Li W, Wang JS. Abnormal bilirubin metabolism in patients with sodium taurocholate

cotransporting polypeptide deficiency. J Pediatr Gastroenterol Nutr 2020;71:e138–e141.
12. Carey MC. Critical tables for calculating the cholesterol saturation of native bile. J Lipid Res 1978;19:945–955.
13. Han J, Liu Y, Wang R, Yang Juncong, Ling V, Borchers CH. Metabolic profiling of bile acids in human and mouse blood by LC–MS/MS in combination with phospholipid-depletion solid-phase extraction. analytical chemistry 2014;87:1127–1136.
14. Qiu Y-L, Gong J-Y, Feng J-Y, eWang R-X, Han J, Liu T, Lu Y, Li-Ting Li, Zhang M-H, Sheps JA, Wang N-L, Yan Y-Y, Li J-Q, Chen L, Borchers CH, Sipos B, Knisely AS, Long V, Xing Q-H, Wang J-S. Defects in myosin VB are associated with a spectrum of previously undiagnosed low γ-glutamyltransferase cholestasis. Hepatology 2017;65:1655–1669.
15. Xie G, Wang Y, Wang X, Zhao A, Chen T, Ni Y, Wong L, Zhang H, Zhang J, Liu C, Liu P, Jia W. Profiling of serum bile acids in a healthy chinese population using UPLC–MS/MS. J Proteome Res 2015;14:850–859.
16. Oude Elferink RP, Ottenhoff R, van Wijland M, Smit JJ, Schinkel AH, Groen AK. Regulation of biliary lipid secretion by mdr2 P-glycoprotein in the mouse. J Clin Invest 1995;95:31–38.
17. Gomez-Ospina N, Potter CJ, Xiao R, Manickam K, Kim MS, Kim KH, Shneider BL, Picarsic JL, Jacobson TA, Zhang J, He W, Liu P, Knisely AS, Finegold MJ, Muzny DM, Boerwinkle E, Lupski JR, Plon SE, Gibbs RA, Eng CM, Yang Y, Washington GC, Porteus MH, Berquist WE, Kambham N, Singh RJ, Xia F, Enns GM, Moore DD. Mutations in the nuclear bile acid receptor FXR cause progressive familial intrahepatic cholestasis. Nat Commun 2016;7:10713.
18. He W, Ren B, Mao F, Jing Z, Li Y, Liu Y, Peng B, Yan H, Qi Y, Sun Y, Guo J-T, Sui J, Wang F, Li W. Hepatitis D virus infection of mice expressing human sodium taurocholate co-transporting polypeptide. PLOS Pathogens 2015;11:e1004840.

Received December 28, 2019. Accepted September 2, 2020.

Correspondence
Address correspondence to e-mail: jshwang@shmu.edu.cn; liwenhui@nibs.ac.cn.

Acknowledgments
The authors thank their patients for their participation in this study.

Conflicts of interest
The authors disclose no conflicts.

Funding
This work was supported by National Natural Science Foundation of China grants 81525018 (W.L.) and 81570468 (J.-S.W.), Science and Technology Major Project of Beijing grant D171100003117003 (W.L.), Shanghai Medical Key Subject Construction Project grant ZK2015A04 (J.-S.W.), and the Science and Technology Bureau of the Beijing Municipal Government (W.L. and J.S.).